

1 **An aptamer-mediated base editing platform for simultaneous knock-in and multiple gene**  
2 **knockout for allogeneic CAR-T cells generation**

3 Immacolata Porreca<sup>1</sup>, Robert Blassberg<sup>1</sup>, Jennifer Harbottle<sup>1,‡</sup>, Bronwyn Joubert<sup>1</sup>, Olga Mielczarek<sup>1</sup>, Jesse  
4 Stombaugh<sup>1</sup>, Kevin Hemphill<sup>1</sup>, Jonathan Sumner<sup>2</sup>, Deividas Pazeraitis<sup>2</sup>, Julia Liz Touza<sup>2</sup>, Margherita  
5 Francesatto<sup>2</sup>, Tommaso Selmi<sup>1,‡</sup>, Juan Carlos Collantes<sup>3</sup>, Zaklina Strezoska<sup>1</sup>, Benjamin Taylor<sup>2</sup>, Shengkan  
6 Jin<sup>4</sup>, Ceri M Wiggins<sup>1,†</sup>, Anja van Brabant Smith<sup>1</sup>, John J. Lambourne<sup>1, ¶</sup>

7 1 Revvity, Cambridge

8 2 AstraZeneca, Discovery Sciences, R&D, Cambridge

9 3 Departamento de Biotecnología, Colegio de Ciencias Biológicas y Ambientales, Universidad San  
10 Francisco de Quito, Campus Cumbayá, Casilla Postal 17-1200-841, Quito 170901, Ecuador.

11 4 Pharmacology Department, Rutgers-the State University of New Jersey, Robert Wood Johnson Medical  
12 School, 675 Hoes Lane West, Piscataway, NJ 08854, USA

13 ‡ Current Address: AstraZeneca, Safety Sciences, Cell Therapy Oncology team, R&D, Cambridge, UK

14 † Current Address: AstraZeneca, Cambridge, UK

15 ‡ Current Address: Consiglio Nazionale delle Ricerche, Istituto di Tecnologie Biomediche, Via Fratelli Cervi 93,  
16 20054 Segrate (MI), IT

17 ¶ Current Address: Transine Therapeutics, Cambridge, UK

18 Correspondence should be addressed to I.P. ([immacolata.porreca@horizondiscovery.com](mailto:immacolata.porreca@horizondiscovery.com), +44 (0) 1223  
19 976 000, 8100 Cambridge Research Park, Waterbeach, Cambridge, CB25 9TL, United Kingdom)

20

21

22

23 **Abstract**

24 Gene editing technologies hold promise for enabling the next generation of adoptive cellular  
25 therapies. Conventional gene editing platforms that rely on nuclease activity, such as Clustered  
26 regularly interspaced short palindromic repeats-CRISPR associated protein 9 (CRISPR-Cas9),  
27 allow efficient introduction of genetic modifications; however, these modifications occur via the  
28 generation of DNA double-strand breaks (DSBs) and can lead to unwanted genomic alterations  
29 and genotoxicity. Here, we apply the novel modular RNA aptamer-mediated Pin-point™ base  
30 editing platform to simultaneously introduce multiple gene knockouts and site-specific  
31 integration of a transgene in human primary T cells. We demonstrate high editing efficiency and  
32 purity at all target sites and significantly reduced frequency of chromosomal translocations  
33 compared to the conventional CRISPR-Cas9 system. Site-specific knock-in of a chimeric antigen  
34 receptor (CAR) and multiplex gene knockout are achieved within a single intervention and  
35 without the requirement for additional sequence-targeting components. The ability to perform  
36 complex genome editing efficiently and precisely highlights the potential of the Pin-point  
37 platform for application in a range of advanced cell therapies.

38

## 39 **Introduction**

40 Gene editing technologies have entered the clinic and show significant potential for advancing  
41 next generation therapies, particularly in the development of more efficient CAR-T cell therapies  
42 to address hematological malignancies<sup>1-3</sup>. To overcome the logistical and infrastructure-related  
43 challenges and product variability barriers of the autologous cell therapy paradigm, recent focus  
44 has shifted to realising the potential of allogeneic cell therapies. The manufacture of allogeneic  
45 cell products requires multiple edits to prevent both graft-versus-host disease and immune  
46 rejection by the host, which would otherwise limit efficacy and persistence of the cell product.  
47 To expand the scope of these innovative off-the-shelf therapies to solid tumors, further edits will  
48 also be required to ensure therapeutic cells retain their efficacy in the refractory and  
49 heterogeneous tumor microenvironment<sup>4</sup>. These factors, together with the need to provide new  
50 functions to the cells to make effective and safe therapies that offer wider patient accessibility  
51 and therapy deployment, ultimately demand increasingly refined editing strategies.

52 Gene editing technologies such as zinc finger nucleases (ZFN), transcription activator-like  
53 effector nucleases (TALEN) and CRISPR-Cas9 have all been employed to successfully perform  
54 targeted editing at genomic loci for effective knockout and knock-in applications. However, the  
55 generation of DSBs inherent to their mechanism of conferring a DNA edit brings concerns of  
56 potentially deleterious mutagenic events<sup>5-11</sup>. The occurrence of chromosomal aberrations is  
57 enhanced in the context of multi-gene editing as more concurrent DSBs are generated, and the  
58 extent of this damage is expanded if DNA breaks also occur at off-target sites. Although many  
59 structural aberrations in a cell may not be viable, it has been reported that some

60 rearrangements could be stable and persist over time <sup>1,9</sup>, potentially increasing the  
61 tumorigenicity risk and compromising the safety of engineered cell therapy products.

62 Base editing with its ability to induce genetic modifications without relying on DSB formation<sup>12,13</sup>  
63 has emerged as a strong contender in the development of advanced cell therapies, particularly  
64 in the context of multi-gene editing strategies. The two main categories of base editors, cytosine  
65 base editors (CBE) and adenine base editors (ABE) mediate efficient C to T and A to G base  
66 changes, respectively<sup>12,13</sup>. Due to their capacity for programmable introduction of a single point  
67 mutation, base editors have been employed to facilitate gene disruption via generation of a  
68 premature termination codon (PTC)<sup>14,15</sup> or by mutation of splice acceptor (SA) or splice donor  
69 (SD) sites at exon-intron boundaries <sup>16,17</sup> with high precision and efficiency whilst generating  
70 minimal undesired editing outcomes compared with standard nucleases. Rapid technological  
71 developments to increase the precision, efficiency and targeting scope of base editors, alongside  
72 an improved safety profile<sup>16,18,19</sup>, have enabled fast-tracked and successful progression to the  
73 clinic<sup>20</sup>. While multiple gene knockouts in immune cells have been successfully achieved by base  
74 editing <sup>16,18,19,21</sup>, more complex genetic modifications, such as targeted transgene integration  
75 alongside base editing knockout at other loci, have only been shown by combining two  
76 orthogonal Cas enzymes<sup>19,22</sup>.

77 We have previously described the modular RNA aptamer-mediated Pin-point base editing  
78 system and demonstrated that this technology can edit targeted cytosines with high efficiency in  
79 human immortalized cells<sup>23</sup>. The Pin-point technology (Figure 1A) relies on a CRISPR-Cas module  
80 and a recruiting RNA aptamer derived from the operator stem-loop of bacteriophage MS2 (MS2)  
81 fused to the guide RNA (gRNA) to recruit the effector module. The effector module is composed

82 of a deaminase (e.g. rAPOBEC1) fused to MS2 coat protein (MCP), which binds to the MS2  
83 aptamer. The recruitment of the deaminase to the target site results in editing of specific  
84 residues on the unpaired DNA strand within the CRISPR R-loop.

85 We demonstrate the adaptation of the plasmid-based Pin-point system<sup>23</sup> into a safe and  
86 efficient fully synthetic system which can be readily adopted for manufacturing engineered cell  
87 therapies by combing mRNAs encoding the requisite Cas and deaminase modules with Pin-point  
88 gRNAs. We utilize a Pin-point base editor composed of rAPOBEC1 and Cas9 nickase (nCas9) for  
89 the generation of allogeneic human CAR-T cells. Initially, we performed a screen to identify  
90 highly functional aptamer-containing guide RNAs (gRNAs) targeting four well established genes  
91 capable of enhancing CAR-T cell function: beta-2-microglobulin (*B2M*), T cell receptor alpha  
92 constant (*TRAC*), CD52 molecule (*CD52*), and programmed cell death protein 1 (*PDCD1*). We  
93 demonstrate efficient and specific multi-gene editing with minimal differences in editing  
94 efficiencies whether editing a single locus or multiple loci and with undetectable incidence of  
95 chromosomal translocations. In addition to being compatible with conventional lentiviral CAR  
96 transgene delivery technologies the Pin-point gene editing platform can be employed to  
97 perform novel multiplex genome engineering operations, enabling simultaneous target  
98 transgene knock-in and multi targets knockout. We demonstrate the utility of this approach by  
99 combining aptamer-containing and aptamer-less gRNAs to generate functional engineered CAR-  
100 T cells via simultaneous knockout of multiple targets alongside targeted CD19-CAR insertion at  
101 the endogenous TRAC locus. The Pin-point platform thus enables complex genetic modifications  
102 of T cells using a single DNA-targeting nuclease via a novel single-step process.

103

## 104 **Results**

### 105 **Multiplex editing in human T cells with Pin-point base editing system**

106 To determine the optimal Pin-point system configuration with rAPOBEC1 as the effector module  
107 we assessed the impact of aptamer copy number and position within the gRNA on editing  
108 efficiencies in mammalian cells. The configuration with one copy of the MS2 aptamer located at  
109 the 3' end of the tracrRNA resulted in optimal base editing across multiple loci (Figure S1) and  
110 was adopted as the basis for the synthetic gRNA designs employed in this study.

111 Using fully synthetic RNA reagents, as is conventional in engineered adoptive T cell therapy  
112 manufacturing, we screened a panel of crRNAs to identify the best performing gRNAs for  
113 knockout of *B2M*, *TRAC*, *PDCD1*, and *CD52* with the Pin-point base editing system. The crRNAs  
114 were designed to result in the introduction of a PTC or mutation at either the SA or SD sites in  
115 each target gene (Table S1). Individual crRNAs were delivered into human primary T cells by  
116 electroporation in combination with the aptamer-containing tracrRNA, an mRNA encoding  
117 nCas9 fused to a uracil glycosylase inhibitor (UGI) and an mRNA encoding rAPOBEC1-MCP. Base  
118 conversion was assessed by amplicon sequencing and target protein expression was evaluated  
119 by flow cytometry (Figure S2A-B). crRNAs exhibiting the highest level of target C to T conversion  
120 and associated protein loss for each gene (SD disruption in exon 1 for *B2M*, SD disruption in  
121 exon 1 for *CD52*, SA disruption in exon 3 for *TRAC* and SD disruption in exon 1 for *PDCD1*) were  
122 selected for synthesis as one-part single gRNAs (sgRNA) for simultaneous multi-gene editing.  
123 Delivery of sgRNAs in multiplex achieved high levels of C to T conversion at each of the four  
124 target genes (~76%-85%) (Figure 1B) with efficiencies comparable to that observed for individual  
125 sgRNA delivery (Figure S2C). We observed minimal undesired C to A or C to G conversion (Figure

126 1B-C and Figure S3A) or indel mutations (Figure 1D and Figure S3B) at each of the 4 target loci.  
127 Thus, the Pin-point system configuration consisting of nCas9 containing UGI, rAPOBEC1-MCP  
128 and an sgRNA containing an MS2 aptamer is capable of simultaneously generating C to T edits  
129 with high efficiency and purity at multiple target loci when delivered to human T cells by  
130 synthetic RNA reagents.

### 131 **Characterization of multi-gene knockout T cells**

132 To determine the extent of multiplex target protein knockout in individual cells we performed  
133 multi color flow cytometry analysis. Consistent with the high base editing efficiency we observed  
134 at the genomic level (Figure 1B and Figure S2C), protein expression of each individual target was  
135 reduced by ~75%-85% (Figure 2A). This was comparable to the level of protein knockout  
136 obtained using SpCas9 with sgRNAs designed for optimal indel formation at these loci (Figure  
137 2A). Furthermore, approximately 80% of T cells edited by either the Pin-point system or by  
138 SpCas9 were negative for the three markers TCRa/b, B2M and CD52 while the remaining 20%  
139 were double negative compared to approximately 80% of mock electroporated T cells from  
140 multiple donors which were positive for all three markers (Figure 2B). PDCD1 requires T cell  
141 activation for optimal expression; therefore, T cells were cultured in the presence of phorbol 12-  
142 myristate 13-acetate (PMA) and ionomycin<sup>24</sup> immediately prior to analysis to enable  
143 simultaneous quantification of all four markers. PMA-ionomycin activated T cells exhibited a  
144 more heterogeneous phenotype than unstimulated T cells due to both non-uniform  
145 upregulation of PD1 and the downregulation of TCRa/b, with ~50% of mock electroporated  
146 controls expressing all four markers and ~35% expressing three of the four markers (Figure S4).  
147 Nonetheless, ~50% of T cells edited by the Pin-point system and ~60% of T cells edited by

148 SpCas9 were negative for the four targets, with an additional 30% negative for three of the four  
149 targets (Figure S4). This indicates a high degree of simultaneous knockout, consistent with the  
150 expectations based on individual target knockout efficiencies.

151 It is well known that nuclease-dependent gene editing technologies have the potential to impair  
152 cell fitness and proliferative capacity due to the activation of DNA-damage responses, which is  
153 exacerbated when introducing multiple DSBs<sup>25,26</sup>. Consistent with the DSB-independent  
154 mechanism of base editing we observed that simultaneous editing at three or four loci with the  
155 Pin-point system did not impact T cell yield compared to SpCas9 where a significant decrease  
156 was observed (Figure 2C). Thus, the use of the Pin-point base editing technology enables  
157 efficient knockout of multiple genes in T cells without impacting cell fitness or therapeutic cell  
158 yields.

#### 159 **Assessment of gRNA specific off-target editing**

160 The potential of gene editing technologies to generate off-target edits is an important  
161 consideration for clinical risk assessment of engineered cell therapies. To experimentally identify  
162 candidate off-target editing sites for each of the four gRNAs, we performed “circularization for  
163 high-throughput analysis of nuclease genome-wide effects by sequencing” (CHANGE-seq) using  
164 SpCas9 on genomic DNA (gDNA) isolated from T cells<sup>27</sup>. The top 100 SpCas9 off-target candidate  
165 sites for each gRNA identified by CHANGE-seq (Table S2) were subsequently validated by  
166 rhAmpSeq in T cells edited at the four target loci using either SpCas9 or the Pin-point system. Of  
167 the 400 CHANGE-seq candidate sites that were analysed, only 2 showed detectable off-target  
168 editing by both SpCas9 and the Pin-point base editing system (1.2%-20% indel frequency and  
169 0.7%-2.2% base editing, respectively), with an additional two sites (one for the CD52 gRNA and  
170 one for the B2M gRNA) that were edited by the Pin-point base editing system only, albeit at very



171 low levels (0.7%-1%) (Figure 3A-B, Table S2). We therefore conclude that multi-gene editing with  
172 the Pin-point system configuration composed of nCas9 and rAPOBEC1 reduces sgRNA-  
173 dependent off-target editing compared to SpCas9.

#### 174 **Assessment of chromosomal translocations**

175 In addition to the generation of undesired edits at off-target DNA sites, multiplex editing with  
176 DSB-dependent technologies can lead to the generation of chromosomal translocations <sup>1,2</sup>.  
177 Because the Cas9 nickase variant used in the Pin-point base editing system cleaves only one DNA  
178 strand <sup>28,29</sup>, we hypothesized that multi-gene editing with the Pin-point base editor would  
179 substantially reduce the occurrence of chromosomal translocations. To test this, we performed  
180 targeted DNA capture to enrich for genomic regions around the four gRNA target sequences,  
181 followed by paired-end sequencing to an average depth of 4000X (Capture-seq) (Table S3).  
182 Identification and quantification of translocations for each target was performed using the  
183 DRAGEN Structural Variant (SV) Caller<sup>30 31</sup> (Figure 3C and Table S4). To validate the Capture-seq  
184 method, translocations between the four target genes were quantified by orthogonal droplet  
185 digital polymerase chain reaction (ddPCR) analysis using probes spanning the expected  
186 translocation breakpoints. Translocations were identified at comparable frequencies using the  
187 two methods (Figure S5A). We consistently detected all expected on-target to on-target  
188 translocation events with frequencies ranging between 0.2%-1.6%, and translocations between  
189 gRNA target regions and the PDCD1-associated off-target site identified by CHANGE-seq in the  
190 SpCas9 multi-edited samples (Figure S5B-C, Table S4), further confirming it as a contributor to  
191 CRISPR-Cas9-mediated genome instability. Frequencies of these SpCas9 induced translocations  
192 persisted over time while remaining undetectable in samples edited with the Pin-point system

193 (Figure S5C). In summary, the aggregation of translocation frequencies quantified from T cells  
194 edited at four loci with SpCas9 (2-3%, Table S4) indicates that 1 in 33-50 haploid genomes (up to  
195 1 in 17-25 diploid cells) will potentially carry a translocation event, while these types of  
196 chromosomal abnormalities are unlikely to occur in cells edited with the Pin-point system. Thus,  
197 multi-gene editing with the Pin-point system greatly reduces the adverse effects on genome  
198 stability associated with SpCas9.

### 199 **Molecular assessment of RNA deamination**

200 As promiscuous activity of the deaminase component of base editors has the potential to  
201 deaminate RNA<sup>32,33</sup> similarly to the activity of endogenous cellular deaminases<sup>34</sup>, we assessed  
202 the impact on cytidine deamination of RNA by performing transcriptome-wide messenger RNA-  
203 sequencing (mRNA-Seq). Previous findings have highlighted that thousands of C to U transitions  
204 occur throughout the transcriptome when base editors are delivered in plasmid format<sup>32,33,35</sup>. To  
205 evaluate the impact on RNA deamination of the more therapeutically relevant RNA-based  
206 transient expression of the Pin-point system in human primary T cells, we performed an mRNA-  
207 Seq time course (day 1, 3 and 7 post-electroporation) and observed a low-level, transient, gRNA-  
208 independent increase in RNA deamination events compared to nCas9-UGI-UGI alone  
209 (approximately 60 additional C to U transitions observed exclusively at day 1 post-  
210 electroporation) (Figure 4A, B). Consistent with these observations, the level of mRNAs encoding  
211 the different components of the Pin-point base editing platform rapidly declines, becoming  
212 undetectable by day 7 in culture (Figure 4C).

### 213 **Phenotypic analysis of edited T cells**

214 We investigated whether the transient mRNA deamination associated with base editing with the  
215 Pin-point system had any major effects on the gene expression profile of T cells by performing  
216 differential gene expression analysis on the mRNA-Seq time course dataset. Global gene  
217 expression was minimally affected by the delivery of Pin-point mRNAs and a non-targeting  
218 sgRNA (175, 142 and 2 transcripts were deregulated, up- or down-regulated, at day 1, 3 and 7,  
219 respectively) (Figure 4D-F and Table S5). We observed a similar effect on the transcriptome  
220 when the four gene specific sgRNAs were delivered (123, 350 and 66 transcripts were  
221 deregulated at day 1, 3 and 7, respectively) (Figure 4G-I and Table S5), indicating that the major  
222 component of the effect on gene expression profile is gRNA sequence independent.

223 In line with expectations five transcripts encoding the sgRNA targets B2M, PDCD1, CD52, a  
224 miRNA (MIR10393) associated with the B2M gene, and a non-coding and uncharacterized gene  
225 associated with the PDCD1 gene (LOC105373977) were stably downregulated in the samples  
226 edited with the 4 gene specific sgRNAs (Figure S6 and Table S5) whereas none of the  
227 differentially expressed transcripts were stably deregulated across the time course of samples  
228 edited with the non-targeting sgRNA. Of the deregulated genes, 41 were deregulated in both  
229 targeted and untargeted conditions one day after electroporation and 56 were deregulated in  
230 both conditions at day 3 (Figure S6). These transient gene expression changes likely reflect an  
231 immediate cellular response to the delivery of exogenous RNAs or occurred as a consequence of  
232 the transient RNA deamination events described above. In conclusion, we observed low level  
233 and transient RNA deamination by base editing using the Pin-point system that did not result in  
234 a significant long-term perturbation of the T cells transcriptional identity.

235 **Generation of allogeneic CAR-T cells by multi-gene editing with the Pin-point system and**  
236 **lentiviral delivery of the CAR**

237 Having established that synthetic RNA-based delivery of the Pin-point base editing system  
238 presented minimal detrimental effects on human primary T cells, we employed the system to  
239 generate allogeneic CAR-T cells. We first sought to prove the compatibility of gene editing using  
240 the Pin-point system with the industry standard lentiviral CAR transgene delivery approach<sup>36</sup>.  
241 Human primary T cells were first transduced with a lentivirus to deliver the CD19-CAR and then  
242 edited at the four target genes by electroporation of mRNA encoding either the Pin-point  
243 system or SpCas9 and the appropriate targeting gRNAs for *B2M*, *CD52*, *PDCD1* and *TRAC*. High  
244 efficiency protein depletion for all four targets (60-80%) was achieved, comparable to results  
245 obtained with SpCas9 (Figure 5A) without interfering with CD19-CAR expression (Figure 5B). The  
246 multi-gene edited CAR-T cells generated with the Pin-point base editing system retained the  
247 ability to kill antigen positive cancer cells in vitro (Figure 5C) and to produce the effector  
248 cytokines TNF $\alpha$  and IFN $\gamma$  (Figure 5D) with efficiency comparable to SpCas9 edited and unedited  
249 control CAR-T cells.

#### 250 **Generation of allogeneic CAR-T cells by multi-gene editing and simultaneous site-specific** 251 **knock-in of the CAR with Pin-point system**

252 In contrast to lentiviral delivery, targeted insertion of a CAR transgene can result in a more  
253 homogeneous cell therapy with improved functionality<sup>37</sup> and reduced insertional oncogenesis  
254 risk. We therefore developed site-specific knock-in using the Pin-point platform by exploiting the  
255 aptamer-dependent deaminase recruitment, to achieve simultaneous multiplex gene knockout  
256 and CD19-CAR knock-in in a single event (Figure 6A). The sgRNAs containing aptamers recruit  
257 the entire Pin-point base editing machinery to the target site intended to be base edited (Figure  
258 6A, left), while the use of two consecutive aptamer-less sgRNAs enables the recruitment of two

259 nCas9 molecules alone at the knock-in site (Figure 6B, right) allowing to direct discreet functions  
260 to specific loci. Firstly, we verified that the deaminase expression did not affect the efficiency of  
261 site-specific knock-in of a GFP reporter or of CD19-CAR at the *TRAC* locus by the nCas9  
262 component of the Pin-point base editing system (Figure S7A and S7B respectively).  
263 Subsequently, we performed multiplex base editing using the Pin-point platform with  
264 simultaneous site-specific knock-in of CD19-CAR at the *TRAC* locus. Primary human T cells were  
265 electroporated with mRNAs encoding nCas9 and rAPOBEC1-MCP, aptamer-containing gRNAs  
266 directed to base edit *B2M*, *CD52* and *PDCD1*, and two aptamer-less gRNAs designed to target  
267 nCas9 alone to exon 1 of the *TRAC* locus to enable homology-directed repair (HDR) driven  
268 integration of the CD19-CAR. A CD19-CAR transgene lacking a promoter flanked by sequences  
269 homologous to the *TRAC* locus was then delivered by AAV6 particles. We achieved high levels  
270 (60-90%) of protein depletion for both the base editing targets (B2M, CD52 and PD1) and the  
271 integration target (TRAC) (Figure 6B). The level of site-specific knock-in evaluated by CD19-CAR  
272 expression from the endogenous TRAC locus using the simultaneous knock-in knockout  
273 application of the Pin-point system was comparable to the results achieved with SpCas9 (~20%)  
274 (Figure 6C). Moreover, CAR-T cells generated by simultaneous knock-in and knockout using the  
275 Pin-point system were functional, showing comparable ability to kill antigen positive target cells  
276 in vitro (Figure 6D) and produce the effector cytokines TNF $\alpha$  and IFN $\gamma$  (Figure 6E) as SpCas9  
277 engineered controls.  
278 These data demonstrate that the Pin-point system is a promising technology for simultaneous  
279 multiplex gene editing and targeted gene insertion applications, while limiting the deleterious  
280 effects of nuclease-dependent gene editing. Furthermore, the ability to efficiently base edit  
281 multiple sites while allowing targeted integration without the requirement of additional

282 orthogonal targeting enzymes in a single editing procedure is unique to the Pin-point platform  
283 and has large potential in the development of complex, engineered cell and gene therapy  
284 products.

285

286

## 287 Discussion

288 We present the first proof of functionality of the Pin-point system in primary human T cells,  
289 demonstrating that the technology can be employed to simultaneously introduce base edits at  
290 multiple loci at high efficiency in combination with site-specific transgene integration in a single  
291 intervention. When applied to the generation of engineered CAR-T cells using fully synthetic  
292 RNA components the Pin-point system exhibits a favourable safety profile compared to DSB-  
293 dependent CRISPR-Cas9 technology. Unbiased identification of candidate gRNA-dependent Cas9  
294 off-target editing sites<sup>27</sup> revealed the Pin-point base editing system to be highly specific with  
295 only 4 out of 400 analysed sites showing editing. When editing four targets simultaneously with  
296 SpCas9 we detected translocations at frequencies where 1 in every 17-25 cells of the final  
297 product would likely contain a translocation. Translocations were undetectable with the Pin-  
298 point technology, as it has been previously reported using other base editors<sup>16,18,19</sup>. Multi-gene  
299 editing with the Pin-point system also improved engineered T cell yield compared to SpCas9,  
300 presenting an advantage for the manufacturing of both autologous and allogeneic therapies by  
301 increasing the yield of therapeutic product per volume of donated blood, ultimately reducing  
302 cost, opening the potential to make available at a lower price and broadening access.

303 Base editing combined with lentiviral delivery of the CAR transgene has been applied for  
304 multiple gene knockout for the generation of enhanced allogeneic CAR-T therapy<sup>16,18,19,21 36</sup>,  
305 however such approaches come with many limitations, including the risk of insertional  
306 mutagenesis, variable transgene expression and gene silencing. To overcome these limitations,  
307 targeted transgene integration facilitated by CRISPR-Cas technologies has become increasingly  
308 popular<sup>38</sup>. However, to date, simultaneous site-specific knock-in alongside base editing at other

309 loci has only been achieved by combining two Cas homologs (i.e. Cas9 for base editing and Cas12  
310 for knock-in) to avoid cross utilisation of sgRNAs<sup>19,22</sup>. The aptamer-dependent nature of the Pin-  
311 point system overcomes this requirement for the delivery of multiple large Cas enzymes by  
312 independently controlling which active modules are recruited at each of multiple target loci.  
313 Whereas aptamer containing gRNAs recruit the complete base editing machinery consisting of  
314 the nCas9 and the deaminase modules to loci intended for gene knockout via base conversion,  
315 aptamer-less gRNAs recruit only the nCas9 module to loci intended for transgene insertion but  
316 avoid recruiting the deaminase function, which could otherwise induce deamination at the  
317 integration site.

318 Although the aptamer-dependent design of the Pin-point base editing system has the advantage  
319 of increased flexibility, the untethered deaminase could in principle increase the risk of spurious  
320 deamination. We addressed concerns about rAPOBEC1 mediated deamination<sup>33,35</sup> and  
321 determined that delivery of the Pin-point base editing machinery in the form of synthetic  
322 reagents into human primary T cells resulted in transient deamination of a minor fraction of  
323 expressed mRNAs. Nonetheless, all off-target alterations to the transcriptome rapidly dissipated  
324 and would therefore not affect the phenotype of T cells at the point of infusion of the allogeneic  
325 product. Taken together with the marked improvements in genome stability and yield of multi-  
326 gene edited T cell we propose that the Pin-point system represents a substantive advance in the  
327 toolkit available for safely engineering complex adoptive cellular therapies.

328 Due to its inherent flexibility, we anticipate that the Pin-point platform could be configured to  
329 simultaneously perform a suite of independent operations at multiple genomic loci by recruiting  
330 the desired effector modules via distinct RNA aptamers. For example, by combining deaminase



331 and epigenetic modulation modules it should be possible to rewire gene regulatory networks to  
332 confer novel T cell responses to stimuli by simultaneously modifying the sequence of cis-  
333 regulatory elements and the chromatin organisation at specific loci in combination with the site-  
334 specific incorporation of synthetic signalling receptors. Similarly, it should be possible to rewire  
335 metabolic networks to overcome challenges such as T cell exhaustion by rationally engineering  
336 the activity of key enzymes in situ by base editing while simultaneously inducing or reducing  
337 expression of additional endogenous metabolic enzymes using transcriptional activator or  
338 repressor modules. Beyond its application in the creation of next-generation adoptive T cell  
339 therapies we anticipate the Pin-point system will offer similar opportunities for the engineering  
340 of a wide range of allogeneic cell therapies with increasingly advanced safety and functionality  
341 profiles.

## 342 **Material and methods**

### 343 **Guide RNA design**

344 gRNAs for base editing have been designed by using an internal design tool for PTCs generation or by  
345 manual design for the splice site disruption. The internal tool searches for NGG PAM within exons and  
346 20bp protospacer sequences that include a C in positions 2-18 that when converted to T introduce a  
347 STOP codon. For splice site disruption, the approach was based on editing the conserved splice  
348 acceptor (intron-AG|exon) or splice donor (exon|GT-intron) motif to disrupt the functional transcript.  
349 This was done by finding an NGG PAM site near the splice junction and 20 bp protospacer that  
350 included the splice acceptor or donor site to edit. Guides that targeted more than a single location  
351 within the genome were removed from consideration. Guide RNA information for base editing is

352 reported in Table S1. Information regarding gRNAs utilized with SpCas9 for optimal indels  
353 formation<sup>37,39,40</sup> are reported in Table S6.

354 For the knock-in strategy we designed two gRNAs (Table S7) with PAM-out configuration to target  
355 opposite strands in the first exon of the TRAC gene. Both, non-homologous end joining (NHEJ) and  
356 integration of the CAR by HDR at this locus has been proven to efficiently disrupt the TCR complex<sup>37</sup>.

### 357 **Editing reagents**

358 Pin-point system (nCAs9-UGU-UGI and rAPOBEC1-MCP) and SpCas9 mRNAs were produced  
359 commercially (Trilink Biotechnologies and Horizon Discovery<sup>TM</sup>). Sequences are available in  
360 Supplemental material. Guide RNA reagents (crRNAs, tracrRNA and sgRNAs) were synthesized at  
361 Horizon<sup>TM</sup>, a PerkinElmer<sup>TM</sup> company, or at Agilent Technologies.

### 362 **Primary human T cell isolation and culture**

363 Primary human T cells (CD3+) were either purchased (Hemacare, CA, USA), or isolated in-house from  
364 fresh whole peripheral blood (CPD blood bags, Cambridge Bioscience, UK) or Leukopak (BioIVT) from  
365 healthy donors in accordance with Human Tissue Act (HTA) regulations. Peripheral blood mononuclear  
366 cells (PBMC) were isolated by density gradient centrifugation with Lymphoprep (StemCell Technologies,  
367 Germany) in SepMate-50 (StemCell Technologies, Germany) tubes. T cells were subsequently isolated  
368 from the PBMC population by immunomagnetic negative selective with the EasySep Human T Cell  
369 Isolation kit (StemCell Technologies, Canada). Isolated T cells with >95% viability and >95% purity were  
370 either cryopreserved or directly cultured for subsequent experiments. T cells were cultured at ~1-2 x  
371 10<sup>6</sup>mL in ImmunoCult-XF T cell expansion medium (StemCell Technologies, Canada) supplemented with  
372 Penicillin-Streptomycin (Gibco, NY, USA) and IL-2 (100 IU/mL; Miltenyi Biotech). Cells were activated

373 with Dynabeads Human T-Activator CD3/CD28 (Gibco, Vilnius, Lithuania) at a 1:1 bead:cell ratio for 48 h  
374 prior to electroporation.

### 375 **T Cell Electroporation**

376 After activation, Dynabeads were magnetically removed and the cells were washed with Dulbecco's  
377 PBS (Gibco, Paisley, UK) prior to resuspension in the electroporation Buffer R. Activated T cells (2.5 x  
378 10<sup>5</sup> per reaction) were electroporated with sgRNAs at 2uM or with tracrRNA/crRNA at 6 uM and either  
379 1 µg of SpCas9 mRNA or 1.6 µg of Pin-point nCas9-UGI-UGI and 0.2 µg of Pin-point rApobec1 using the  
380 Neon Transfection System (Invitrogen, South Korea) with the 10 µL tips and the following conditions:  
381 1600 volts, pulse width of 10 ms, 3 pulses. After electroporation, T cells were transferred directly to  
382 prewarmed antibiotic-free ImmunoCult-XV T cell expansion medium supplemented with IL-2 (100  
383 IU/ml), IL-7 (100 IU/ml; Peprotech, New Jersey, USA) and IL-15 (100 IU/ml; Peprotech, New Jersey,  
384 USA) and incubated at 37°C, 5% CO<sub>2</sub> for 3-7 days. Electroporations were performed in duplicate or  
385 triplicate for each condition.

### 386 **Lentiviral transduction**

387 Lentivirus was generated in HEK293T cells using Lipofectamine 3000 Transfection Reagent  
388 (Invitrogen), the ViraSafe Lentiviral Packaging System (Cell Biolabs) and an expression plasmid to  
389 deliver the 1928z CAR used in clinical trials (CD19-CAR)<sup>41</sup>. Viral particles were harvested from the  
390 culture, concentrated using 100 kDa Amicon® Ultra-15 Centrifugal Filter Units (Merck) and  
391 cryopreserved at -80°C. Functional viral titre was estimated by titrating the viral particles on Jurkat  
392 cells. Prior to lentiviral transduction, T cells were cultured in ImmunoCult-XV T cell expansion medium  
393 supplemented with human serum (10%; Sigma, USA), Penicillin-Streptomycin and IL-2 (100 IU/ml) and  
394 activated for 24 h in the presence of plate-bound anti-CD3 antibody (2.5 µg/mL; BioLegend) and

395 soluble anti-CD28 antibody (2.5 µg/mL; BioLegend). Cells were transduced on RetroNectin (100  
396 µg/mL; Takara)-coated plates at an MOI of 5 and the transduced population was enriched by  
397 puromycin (3 µg/mL; Gibco, China) selection for 5 days. Cells were then reactivated using Dynabeads  
398 Human T-Activator CD3/CD28 before electroporation with editing reagents as reported above.

### 399 **AAV transduction**

400 The HDR donor sequence is similar to what described by Eyquem et al<sup>37</sup>. In more details, it consists of  
401 1.8Kb of genomic TRAC flanking the left and the right gRNA targeting sequences, a self-cleaving P2A  
402 peptide in frame with the first exon of TRAC and by the 1928z CAR used in clinical trials<sup>41</sup>. The HDR  
403 sequence was cloned by GenScript in an pAAV background, and the resulting plasmid utilized to  
404 generate recombinant AAV6 donor vector by Vigene Bio.

405 For the locus specific knock-in experiment, activated T cells were electroporated with the gRNAs and  
406 Pin-point or SpCas9 mRNAs and immediately after electroporation transduced with the recombinant  
407 AAV6 donor vector at multiplicity of infection of  $5 \times 10^5$ . Subsequently, T cells were cultured in  
408 antibiotic-free ImmunoCult-XV T cell expansion medium supplemented with IL-2 (100 IU/ml), IL-7 (100  
409 IU/ml; Peprotech) and IL-15 (100 IU/ml; Peprotech) at 37°C, 5% CO<sub>2</sub> and culture medium was  
410 completely replaced after 24 hours.

### 411 **Flow cytometry**

412 Prior to flow cytometry, T cells edited only at the PDCD1 locus were re-stimulated using Dynabeads  
413 Human T-Activator CD3/CD28 for 48 h as described above to induce the expression of PD1. In  
414 experiments where the 4 targets were knocked-out, cells were activated with phorbol 12-myristate  
415 13-acetate (PMA; 50 ng/mL; Sigma-Aldrich) and ionomycin (250 ng/mL; Millipore) for 48 hours prior  
416 flow cytometry analysis to induce the expression of PD1. For flow cytometry, cells were stained with

417 fluorophore-conjugated antibodies against human B2M (BioLegend, #316304), CD52 (BD BioSciences,  
418 #562945), TCR a/b (BioLegend, #306742), PD1 (BioLegend, #329908) and CD19-CAR (AcroBiosystems,  
419 anti-FMC63 scFv). Cell viability was assessed using DAPI (80 ng/mL). Cells were acquired on an  
420 IntelliCyte IQue PLUS or Sartorius iQue3 flow cytometer using iQue ForeCyt® Enterprise Client Edition  
421 9.0 (R3) Software for both acquisition and data analysis. The gating strategy for simultaneous  
422 quantification of viability, B2M, CD52, TCR a/b and PD1 expression was as follows (Figure S8). Within  
423 the live population, B2M expression versus CD52 expression was assessed using quadrant gating, then  
424 within each of the 4 subpopulations TCR a/b and PD1 expression was assessed using quadrant gating.  
425 Each of these 16 populations represents a different expression profile of the 4 targets and cell counts  
426 within each population were used to calculate the frequency of cells which had lost each target or  
427 combination of targets.

428 For fold expansion calculation, CountBright Absolute Counting Beads (Invitrogen) were added to flow  
429 cytometry samples to allow counting of the absolute number of live (DAPI negative). A flow cytometry  
430 count was performed 2h after editing (baseline), and a second one 3 days after editing. Fold  
431 expansion was calculated by dividing the live cell count for each sample by its own baseline count.

#### 432 **Amplicon sequencing of genomic DNA samples**

433 Locus-specific primers with Illumina universal adapter were designed to amplify a 250-350 bp site  
434 surrounding the genomic region of interest (Table S8). For gDNA preparation, T cells were lysed using  
435 DirectPCR (cell) (Viagen Biotech, LA, USA) lysis buffer supplemented with proteinase K (10 µg/mL;  
436 Sigma-Aldrich) and heated at 55°C for 30 min, then 95°C for 30 min. The crude lysate was then used for  
437 the first PCR with locus specific primers containing Illumina adapters. Products from the first PCR were  
438 then amplified using Illumina barcoding primers. Following barcoding, PCR samples were pooled and

439 purified using AMPure XP beads (Beckman Coulter). DNA was sequenced by SourceBioScience on  
440 Illumina MiSeq 2 × 300 bp runs (Illumina, San Diego, CA). Illumina, San Diego, CA). Raw FASTQ files were  
441 analyzed against a reference sequence and sgRNA protospacer sequence using a custom pipeline that  
442 was used to count nucleotide substitutions in the base editor window (both expected C:G to T:A  
443 conversions and other substitutions) and indels overlapping the spacer sequence as previously  
444 described<sup>23</sup>.

#### 445 **CHANGE-seq – Off-target discovery.**

446 CHANGE-seq was performed as previously described by Lazzarotto et al.<sup>27</sup> with minimal modifications  
447 on gDNA extracted using the Gentra Puregene Cell Kit (Qiagen) from two independent human T cell  
448 (CD3+) donors, following manufacturer's instructions. Size analysis of resultant HMW (High Molecular  
449 Weight) gDNA was assessed in the Fragment Analyzer (Agilent), and subjected to tagmentation with  
450 customized transposome composed of oCRL225/oCRL226 adaptors and the Hyperactive Tn5  
451 transposase (Diagenode). DNA tagmentation was performed in batches of 4ug, utilizing 17.5ul of the  
452 assembled transposome in a final volume of 200ul, and incubated for 6 minutes at 55° C. Reaction  
453 was quenched by the addition of 200ul of SDS 0.4%, and resultant fragments were assessed on the  
454 Fragment analyzer and quantified by Qubit dsDNA BR Assay kit (ThermoFisher). After gap repair with  
455 Kapa Hi-Fi HotStart Uracil+ DNA Polymerase (KAPA Biosystems) and Taq DNA Ligase (NEB) and  
456 treatment with USER enzyme (NEB) and T4 polynucleotide kinase (NEB), the tagmented DNA was  
457 circularized with T4 DNA Ligase (NEB) and treated with a cocktail of exonucleases containing Plasmid-  
458 Safe ATP-dependent DNase (Lucigen), Lambda exonuclease (NEB) and Exonuclease I (NEB) to degrade  
459 residual linear DNA carryover. Circularized material was then in-vitro cleaved by SpCas9 RNP in  
460 combination with sgRNA. Illumina Universal Adaptor (NEB) was ligated to blunted end after  
461 adenylation, enzymatically treated with USER enzyme (NEB) and amplified with NEBNext Multiplex

462 Oligos for Illumina for 20 amplification cycles. The quality of the amplified and bead-cleaned-up  
463 libraries was determined using a 5300 fragment analyzer with the standard sensitivity NGS kit  
464 (Agilent). Libraries were then pooled, diluted, and denatured according to Illumina's  
465 recommendations and sequenced on NextSeq550 300 cycles kit with a paired-end 2x150  
466 configuration (Illumina). Bioinformatic analysis was performed as described by Tsai et al., 2017<sup>42</sup> with  
467 a minor modification: reads with mapping quality equal to zero were included in the analysis  
468 alongside those passing the MAPQ threshold defined in the pipeline parameters, in order to nominate  
469 putative off-targets located in non-uniquely mappable regions. The pipeline was run with the  
470 following parameters: read\_threshold: 4, window\_size: 3, mapq\_threshold: 50, start\_threshold: 1,  
471 gap\_threshold: 3, mismatch\_threshold: 6, search\_radius: 30.

#### 472 **rhAMpSeq – Off-target validation.**

##### 473 *rhAmpSeq panel design*

474 rhAmpSeq panels were designed for each gene target composing 100 sites with a high degree of  
475 overlap between technical and biological replicates from CHANGE-seq results. Hierarchical site  
476 selection strategy was employed to pick the most likely off-target sites: 1) sites present in both donors  
477 and all replicates, 2) sites in all replicates of one donor, 3) sites in at least two replicates of either  
478 donor, and 4) sites in at least one replicate from one donor. In cases where we had more than 100  
479 sites we prioritized based on the nuclease-read count. The genomic coordinates for on- and off-  
480 targets were then entered into IDT's rhAmpSeq CRISPR analysis portal for assay design and ordering.

##### 481 *rhAmpSeq library preparation*

482 gDNA from non-edited T cells (CD3+) and T cells (CD3+) treated with either the Pin-point system or  
483 SpCas9 was extracted 5 days post electroporation using the Gentra Puregene Cell Kit (Qiagen)  
484 following manufacturer's instructions. rhAmpSeq NGS libraries were then generated as per IDT's

485 rhAmpSeq library preparation protocol. Primary pools, secondary pools and single amplicon  
486 rhAmpSeq reactions were then applied on the extracted gDNA. In target rhAmp PCR 1, the 4x  
487 rhAmpSeq library mix was mixed with ~50-80ng of gDNA and amplified using the following  
488 thermocycling conditions: 95 °C for 10 min; [95 °C for 15 s; 61 °C for 8min] × 14 cycles; 99.5 °C for 15  
489 min; 4 °C hold. The PCR 1 product was purified using Agencourt AMPure XP beads (Beckman Coulter)  
490 and immediately proceeded to the rhAmp PCR 2. In PCR 2, dually indexed Illumina sequencing  
491 libraries were generated using PCR 1 product, mixed with 4x rhAmpSeq library mix 2 and unique i5  
492 and i7 primers (IDT), and amplified using the following thermocycling conditions: 95°C for 3 min; [95°C  
493 for 15 s; 60°C for 30 s; 72°C for 30 s] × 24 cycles; 72°C for 1 min; 4°C hold. The final libraries were  
494 purified using Agencourt AMPure XP (Beckman Coulter), quantified using Qubit 1X dsDNA HS Assay Kit  
495 (ThermoFisher Scientific) and quality was checked by qPCR and on a TapeStation 4200 (Agilent).  
496 Paired-end, 151-bp reads were sequenced using the mid-output 300 cycles kit on the Illumina's  
497 NextSeq 550 platform (Illumina).

#### 498 *Bioinformatic processing of rhAmpSeq data*

499 To deal with non-specific PCR products we first aligned merged reads (using FLASH: Fast Length  
500 Adjustment of SHort reads<sup>43</sup>) to the intended reference sequences for each target (using bwa mem)  
501 and used the alignments produced to identify the variants occurring in each reference (minimum 10  
502 reads and allele frequency 0.01%). From these variants an extended set of reference sequences was  
503 constructed comprising the original reference plus putative variant sequences containing the different  
504 combinations of variants. From this extended set of sequences the ones which differed from the  
505 reference in global pairwise alignment by over 20 (Python Bio.pairwise2.align.globalms with scoring 1  
506 for a match, -1 for a mismatch, 1 gap open, -0.5 gap extend) were considered sufficiently different to  
507 constitute non-specific PCR products. This set was clustered based on pairwise alignment scores



508 within 20, and one representative from each cluster formed a “decoy” sequence to add to the targets  
509 passed to CRISPResso2 (version 2.1.1) in pooled mode with base-editing parameters (-w 20 -wc 1 -be).  
510 Following alignment, CRISPResso2 outputs were processed to identify the base position with the  
511 highest Insertion, Deletion or Base Editing event within the windows of gRNA target site +/- 10 bp per  
512 sample per amplicon. Scripts are available on request.

513

## 514 **Capture-seq**

### 515 *Library preparation*

516 gDNA samples were prepared from T cells (CD3+ ) (Hemacare, CA, USA) using DNeasy Blood and  
517 Tissue Kit (Qiagen). 500-750ng of gDNA were used to prepare paired-end sequencing libraries using  
518 KAPA HyperPlus (Roche) workflow. Briefly, gDNA was purified using HyperPure beads (Roche),  
519 fragmented for 20mins at 37°C, and analyzed using Tapestation to confirm consistent fragmentation.  
520 Following end repair and A-tailing, KAPA universal adapters were ligated to gDNA fragments, products  
521 were cleaned and size selected using 0.8X HyperPure beads (Roche). KAPA Unique Dual Indexed  
522 primers (Roche) were incorporated by PCR (4 cycles) using KAPA HiFi Hotstart ReadyMix (Roche).  
523 Following clean-up with HyperPure beads (Roche) libraries were quantified by Qubit and analyzed on  
524 a Tapestation 4200 (Agilent) to confirm fragment size distribution centred around 350bp.

### 525 *Hybridisation capture probe design*

526 DNA probes (120bp long) complementary to sequences within 200bp regions 5' and 3' of the PAM  
527 sites of gene editing targets were designed using 'Oligo' tool (<https://github.com/jbkerry/oligo>) in  
528 OffTarget configuration. Oligo outputs were manually curated to remove probes with stretches of  
529 homology > 30bp. 4 probes per target were chosen and positioned evenly either side of the PAM site.  
530 5'-biotinylated DNA probes were synthesised by IDT as xGen Custom Hybridization Capture Panels.

531 *Hybridisation capture & sequencing*

532 Libraries were enriched for genomic regions flanking gene editing targets using xGen Hybridization  
533 Capture (IDT) workflow. Briefly, 1ug of each indexed library were pooled and ethanol precipitated  
534 with COT DNA, resuspended in xGen Hybridisation Buffer (IDT) containing xGen Universal Blockers TS  
535 Mix (IDT) and 5'-biotinylated custom DNA probes (IDT), heated briefly to 95°C (1 min), and hybridised  
536 overnight at 65°C. Streptavidin conjugated magnetic beads (IDT) were incubated for 45min at 65°C  
537 with the hybridised libraries, immobilised on a magnetic stand, and stringently washed at 65°C.  
538 Following washing, beads were immobilised and captured library fragments were eluted in H<sub>2</sub>O. Post-  
539 capture PCR (12 cycles) was performed using KAPA HiFi Hotstart ReadyMix (Roche) and xGen Library  
540 Amplification Primer Mix (IDT). Following clean-up with HyperPure beads (Roche), target enriched  
541 libraries were quantified by Qubit and analyzed by Bioanalyser to determine fragment size  
542 distribution prior to sequencing. Libraries were diluted to 1.8nM and 2x300bp paired-end reads were  
543 generated on Illumina MiSeq 2 × 300 bp runs (Illumina, San Diego) by Source Bioscience.

544 *Read alignment and structural variant identification*

545 Sequencing reads were trimmed to the first 75bps using a custom Python script and then processed  
546 through the Illumina DRAGEN Structural Variant (SV) Caller<sup>44</sup> (version 3.8.4) to identify structural  
547 variants, which extends the MANTA<sup>45</sup> structural variation pipeline. Each sample was run through the  
548 pipeline as an unpaired tumor sample. An example command is as follows:

```
549 /opt/edico/bin/dragen -f --ref-dir /ephemeral/ucsc.hg38.3.8.4/ --tumor-fastq1  
550 s3://aws_bucket/Sample1_R1_001.paired.75bp.fastq.gz --tumor-fastq2  
551 s3://aws_bucket/Sample1_R2_001.paired.75bp.fastq.gz --output-directory  
552 /ephemeral/DRAGEN_Sample1/ --output-file-prefix Sample1 --enable-duplicate-marking true --enable-
```

553 map-align true --enable-map-align-output true --enable-sv true --RGID-tumor Sample1 --RGSM-tumor  
554 Sample1 --sv-exome true --remove-duplicates true

### 555 *Translocations quantification*

556 To remove reads derived from library fragments captured non-specifically during hybridisation the  
557 “\*.candidateSV.vcf” output from MANTA was first filtered to include only breakends within sequences  
558 mapping to genomic regions +/- 1000bp either side of gene editing targets. Interchromosomal  
559 translocations were quantified by normalising the total count of reads (BND\_PAIR\_COUNT) supporting  
560 a given variant involving regions on two different chromosomes by the total number of reads mapping  
561 to either genomic region fusion point on each chromosome. Where both genomic regions adjacent to  
562 the breakpoint contained sequences targeted by capture probes the average number of reads across  
563 these regions was used for normalisation.

### 564 **Translocation quantification by ddPCR**

565 gDNA samples were prepared from T cells (CD3+) (Hemacare, CA, USA) using DNeasy Blood and Tissue  
566 Kit (Qiagen). qPCR assays were designed to amplify predicted translocation products composed of  
567 sequences flanking each gRNA target site using the Integrated DNA Technologies (IDT) PrimeTime qPCR  
568 probe design tool. Primers and probe information for ddPCR analysis are reported in Table S9. ddPCR  
569 Supermix for Probes (no dUTP) (Bio-Rad) was used for PCR reactions each containing 40-100ng EcoR1  
570 digested gDNA, an internal reference primer pair targeting the PPIA gene + HEX labelled probe (IDT),  
571 and a translocation targeting primer pair + FAM labelled probe (IDT). Droplets were generated and  
572 analysed using the QX200 Droplet-digital PCR system (Bio-Rad) according to manufacturer’s  
573 instructions. Translocation frequency per haploid genome was calculated from two technical replicates  
574 per sample as the fraction of translocation events detected relative to the reference sequence using  
575 QuantaSoft software (Version 1.7.4) (Bio-Rad).

576 **RNA purification and sequencing**

577 Total RNA was isolated from unedited and edited T cells using the RNeasy Mini Kit (Qiagen) and  
578 quality was determined using a BioAnalyser (Agilent) and a NanoDrop Spectrophotometer.

579 Samples were quantified using the RNA assays on the Qubit Fluorometer. Total RNA was  
580 subjected to mRNA isolation and strand-specific RNA sequencing library preparation with the  
581 Illumina Stranded mRNA Prep, Ligation kit according to manufacturer's instructions. The libraries  
582 were validated on the Agilent BioAnalyzer 2100 to check the size distribution of the libraries and  
583 on the Qubit to check the concentration. The RNA sequencing libraries were sequenced on an  
584 Illumina HiSeq X instrument, for an average of minimum 30M 150bp paired end reads per  
585 sample (Source Bioscience).

586 *RNA deamination analysis*

587 RNA sequence variant calling and quality control was performed as described by Grünwald et al<sup>32</sup>. In  
588 short, Illumina paired-end FASTQ sequences were processed through the GATK best practices for  
589 RNA-seq variant calling<sup>46</sup>), which produced analysis-ready BAM files aligned against human hg38  
590 reference genome. RNA variants were called using GATK HaplotypeCaller<sup>47</sup> targeting single nucleotide  
591 variants (SNVs) across chromosomes 1-22, X and Y. Bam-readcount  
592 (<https://github.com/genome/bam-readcount>) was used to quantify per-base nucleotide abundances  
593 per variant.

594 Variant loci in the experimental samples (nCas9-UGI-UGI alone or Pin-point base editor  
595 electroporated cells) were filtered to exclude sites without high confidence reference genotype calls  
596 in the control samples. For a given SNV the read coverage in the control samples (electroporation  
597 control) was set to be above the 90th percentile of the read coverage across all SNVs in the  
598 corresponding experimental samples. Only loci having at least 99% of reads containing the reference

599 allele in the control samples were kept. RNA edits in the experimental samples were filtered to  
600 include only loci with 10 or more reads and with greater than 0% reads containing alternate allele.  
601 Base edits labeled as C-to-U comprise C-to-U edits called on the positive strand as well as G-to-A edits  
602 sourced from the negative strand.

### 603 *Differential gene expression analysis*

604 Sequences were processed through the Illumina DRAGEN RNA Pipeline v3.7.5 to quantify transcripts  
605 per million and read counts. Differential expression analysis was then performed using DESeq2  
606 v1.26.0<sup>48</sup>.

### 607 **Cytotoxicity assay**

608 CD19 expressing Raji cells (InvivoGen #raji-null) were used as target cells in the cytotoxicity  
609 assay. Killing of the target cells was measured by flow cytometry assay or by calcein assay. For  
610 the flow cytometry assay, Raji cells were seeded in 96-well plate ( $5 \times 10^4$ /well) and co-cultured  
611 with T cells stained with CellTrace<sup>TM</sup> Violet (Invitrogen, USA) at the indicated E:T ratios. After 3  
612 days of coculture, cells were stained with LIVE/DEAD<sup>TM</sup> Fixable Near-IR Dead Cell Stain Kit  
613 (Invitrogen, USA) and acquired by flow cytometry. With T cells positive for the CellTrace Violet,  
614 the Raji cells and T cells were gated into distinct populations prior to live-dead analysis. The  
615 percent of viable Raji cells ( $R_{\text{live}}$ ) was used to calculate the percent of T cell-mediated (TCM)  
616 killing as follows:  $\text{TCM killing} = 100 - R_{\text{live}}$ .

617 For the calcein assay, Raji cells were loaded with Calcein AM Dye (Invitrogen) following the  
618 manufacturer's instructions and cocultured in 384-well plate ( $1 \times 10^4$ /well) with T cells at the  
619 indicated E:T ratios. Target cells without effectors served as a negative control and target cells  
620 incubated with 2% Triton X-100 (Merck-Sigma) served as positive control (maximum killing).

621 After 6 h of coculture, culture supernatant was analyzed at the Envision plate reader  
622 (PerkinElmer) with excitation 494 nm and emission 517 nm settings. TCM killing is calculated as  
623 follow:  $\text{TCM killing} = (\text{test condition} - \text{negative control condition}) / (\text{positive control condition} -$   
624  $\text{negative control condition}) * 100.$

### 625 **Cytokine profiling**

626 The MultiCyt® QBeads® PlexScreen Secreted Protein Assay Kit (Sartorius) was used to quantify  
627 the level of tumor necrosis factor alpha (TNF- $\alpha$ ) and interferon gamma (INF- $\gamma$ ) secretion during  
628 the T cell cytotoxicity assays. Protocol D (reduced background, with standard curve) in the  
629 manufacturer's handbook was followed. The IntelliCyt IQue PLUS or Sartorius iQue3 flow  
630 cytometer using iQue ForeCyt® Enterprise Client Edition 9.0 (R3) Software was used for both  
631 acquisition and data analysis, including plotting the standard curves and calculating the absolute  
632 value of each sample. For samples which were diluted prior to analysis, analyte concentration  
633 was multiplied by the dilution factor. Background analyte concentration (Raji alone) was  
634 subtracted from all values and the data plotted using Graph Prism Version 9.4.1 Software.

### 635 **Acknowledgements**

636 S.J. is supported by NJCCR Grant COCR23PRG005 and DOD Grant MD200088. We thank current  
637 Revvity employee Andrea Frapporti for creating the Pin-point system schematics used in the  
638 manuscript. Finally, we thank current and former Revvity colleagues Toby Gould, Sven Hofmann,  
639 Susana Vega, Michael Anbar, Steve Lenger, John McGonigle, Matthew Perkett for their helpful  
640 discussion and support.

### 641 **Author contributions:**

642 IP designed, performed experiments, analyzed data and wrote the manuscript. R.B., J.H., B.J.,  
643 O.M. designed, performed experiments, analyzed data and contributed to the writing. K.H.  
644 designed, performed experiments and analyzed data. J. Stombaugh performed bioinformatic  
645 analysis. J. Sumner, D.P., J.L.Z., M. F. and B. T. led, designed, performed and analysed the  
646 CHANGE-Seq and rhAmpSeq – Off-target validation. Z.S., C.M.W. and A.v.B.S. supervised and  
647 provided critical suggestions. J.C.C., S.J. and T.S. contributed to the ideation of the project. J.C.C.  
648 and S.J. provided critical reagents. J.J.L. led, directed the project and contributed to the writing.  
649 R.B., J.H. and B.J. have contributed equally to the work.

#### 650 **Declaration of interests**

651 M.F, J.L.T, D.P., J.S and B.T are all current or past (while engaged in the research project)  
652 employees of AstraZeneca. I.P., R.B., J.H., B. J., O. M., J. Stombaugh, K.H., T.S., Z.S., C.W., A.v.B.S.  
653 and J.J.L. are current or past (while engaged in the research project) employees at Revvity.  
654 Revvity has an exclusive license from Rutgers University to certain base editing patents.

655

#### 656 **References**

- 657 1. Stadtmayer, E. A. *et al.* CRISPR-engineered T cells in patients with refractory cancer. *Science* **367**,  
658 eaba7365 (2020).
- 659 2. Ottaviano, G. *et al.* Phase 1 clinical trial of CRISPR-engineered CAR19 universal T cells for treatment of  
660 children with refractory B cell leukemia. *Sci. Transl. Med.* **14**, eabq3010 (2022).
- 661 3. Benjamin, R. *et al.* Genome-edited, donor-derived allogeneic anti-CD19 chimeric antigen receptor T cells  
662 in paediatric and adult B-cell acute lymphoblastic leukaemia: results of two phase 1 studies. *The Lancet* **396**,  
663 1885–1894 (2020).

- 664 4. Dimitri, A., Herbst, F. & Fraietta, J. A. Engineering the next-generation of CAR T-cells with CRISPR-Cas9  
665 gene editing. *Mol Cancer* **21**, 78 (2022).
- 666 5. Papathanasiou, S. *et al.* Whole chromosome loss and genomic instability in mouse embryos after  
667 CRISPR-Cas9 genome editing. *Nat Commun* **12**, 5855 (2021).
- 668 6. Alanis-Lobato, G. *et al.* Frequent loss of heterozygosity in CRISPR-Cas9–edited early human embryos.  
669 *Proceedings of the National Academy of Sciences* **118**, e2004832117 (2021).
- 670 7. Zuccaro, M. V. *et al.* Allele-Specific Chromosome Removal after Cas9 Cleavage in Human Embryos. *Cell*  
671 **183**, 1650-1664.e15 (2020).
- 672 8. Leibowitz, M. L. *et al.* Chromothripsis as an on-target consequence of CRISPR–Cas9 genome editing. *Nat*  
673 *Genet* **53**, 895–905 (2021).
- 674 9. Nahmad, A. D. *et al.* Frequent Aneuploidy in Primary Human T Cells after CRISPR-Cas9 cleavage. *Nat*  
675 *Biotechnol* **40**, 1807–1813 (2022).
- 676 10. Boutin, J. *et al.* CRISPR-Cas9 globin editing can induce megabase-scale copy-neutral losses of  
677 heterozygosity in hematopoietic cells. *Nat Commun* **12**, 4922 (2021).
- 678 11. Haapaniemi, E., Botla, S., Persson, J., Schmierer, B. & Taipale, J. CRISPR–Cas9 genome editing induces a  
679 p53-mediated DNA damage response. *Nat Med* **24**, 927–930 (2018).
- 680 12. Komor, A. C., Kim, Y. B., Packer, M. S., Zuris, J. A. & Liu, D. R. Programmable editing of a target base in  
681 genomic DNA without double-stranded DNA cleavage. *Nature* **533**, 420–424 (2016).
- 682 13. Gaudelli, N. M. *et al.* Programmable base editing of A•T to G•C in genomic DNA without DNA cleavage.  
683 *Nature* **551**, 464–471 (2017).
- 684 14. Billon, P. *et al.* CRISPR-Mediated Base Editing Enables Efficient Disruption of Eukaryotic Genes through  
685 Induction of STOP Codons. *Mol Cell* **67**, 1068-1079.e4 (2017).



- 686 15. Kuscu, C. *et al.* CRISPR-STOP: gene silencing through base-editing-induced nonsense mutations. *Nature*  
687 *Methods* **14**, 710–712 (2017).
- 688 16. Webber, B. R. *et al.* Highly efficient multiplex human T cell engineering without double-strand breaks  
689 using Cas9 base editors. *Nat Commun* **10**, 5222 (2019).
- 690 17. Kluesner, M. G. *et al.* CRISPR-Cas9 cytidine and adenosine base editing of splice-sites mediates highly-  
691 efficient disruption of proteins in primary and immortalized cells. *Nat Commun* **12**, 2437 (2021).
- 692 18. Georgiadis, C. *et al.* Base-edited CAR T cells for combinational therapy against T cell malignancies.  
693 *Leukemia* **35**, 3466–3481 (2021).
- 694 19. Diorio, C. *et al.* Cytosine base editing enables quadruple-edited allogeneic CART cells for T-ALL. *Blood*  
695 **140**, 619–629 (2022).
- 696 20. Kingwell, K. Base editors hit the clinic. *Nature Reviews Drug Discovery* **21**, 545–547 (2022).
- 697 21. Gaudelli, N. M. *et al.* Directed evolution of adenine base editors with increased activity and therapeutic  
698 application. *Nat Biotechnol* **38**, 892–900 (2020).
- 699 22. Glaser, V. *et al.* Combining different CRISPR nucleases for simultaneous knock-in and base editing  
700 prevents translocations in multiplex-edited CAR T cells. *Genome Biology* **24**, 89 (2023).
- 701 23. Collantes, J. C. *et al.* Development and Characterization of a Modular CRISPR and RNA Aptamer  
702 Mediated Base Editing System. *The CRISPR Journal* **4**, 58–68 (2021).
- 703 24. Agata, Y. *et al.* Expression of the PD-1 antigen on the surface of stimulated mouse T and B lymphocytes.  
704 *International Immunology* **8**, 765–772 (1996).
- 705 25. van den Berg, J. *et al.* A limited number of double-strand DNA breaks is sufficient to delay cell cycle  
706 progression. *Nucleic Acids Res* **46**, 10132–10144 (2018).

- 707 26. Friskes, A. *et al.* Double-strand break toxicity is chromatin context independent. *Nucleic Acids Research*  
708 **50**, 9930–9947 (2022).
- 709 27. Lazzarotto, C. R. *et al.* CHANGE-seq reveals genetic and epigenetic effects on CRISPR–Cas9 genome-wide  
710 activity. *Nat Biotechnol* **38**, 1317–1327 (2020).
- 711 28. Jinek, M. *et al.* A Programmable Dual-RNA-Guided DNA Endonuclease in Adaptive Bacterial Immunity.  
712 *Science* **337**, 816–821 (2012).
- 713 29. Cong, L. *et al.* Multiplex Genome Engineering Using CRISPR/Cas Systems. *Science* **339**, 819–823 (2013).
- 714 30. Miller, N. A. *et al.* A 26-hour system of highly sensitive whole genome sequencing for emergency  
715 management of genetic diseases. *Genome Medicine* **7**, 100 (2015).
- 716 31. Illumina DRAGEN Bio-IT Platform | Variant calling & genomics software.  
717 <https://www.illumina.com/products/by-type/informatics-products/dragen-bio-it-platform.html>.
- 718 32. Grünewald, J. *et al.* Transcriptome-wide off-target RNA editing induced by CRISPR-guided DNA base  
719 editors. *Nature* (2019) doi:10.1038/s41586-019-1161-z.
- 720 33. Grünewald, J. *et al.* CRISPR DNA base editors with reduced RNA off-target and self-editing activities. *Nat*  
721 *Biotechnol* **37**, 1041–1048 (2019).
- 722 34. Lerner, T., Papavasiliou, F. N. & Pecori, R. RNA Editors, Cofactors, and mRNA Targets: An Overview of the  
723 C-to-U RNA Editing Machinery and Its Implication in Human Disease. *Genes (Basel)* **10**, 13 (2018).
- 724 35. Zhou, C. *et al.* Off-target RNA mutation induced by DNA base editing and its elimination by mutagenesis.  
725 *Nature* **571**, 275–278 (2019).
- 726 36. Vormittag, P., Gunn, R., Ghorashian, S. & Veraitch, F. S. A guide to manufacturing CAR T cell therapies.  
727 *Curr Opin Biotechnol* **53**, 164–181 (2018).

- 728 37. Eyquem, J. *et al.* Targeting a CAR to the TRAC locus with CRISPR/Cas9 enhances tumour rejection.  
729 *Nature* **543**, 113–117 (2017).
- 730 38. Roth, T. L. *et al.* Pooled Knockin Targeting for Genome Engineering of Cellular Immunotherapies. *Cell*  
731 (2020) doi:10.1016/j.cell.2020.03.039.
- 732 39. Barkal, A. A. *et al.* Engagement of MHC class I by the inhibitory receptor LILRB1 suppresses macrophages  
733 and is a target of cancer immunotherapy. *Nat Immunol* **19**, 76–84 (2018).
- 734 40. Kamali, E., Rahbarizadeh, F., Hojati, Z. & Frödin, M. CRISPR/Cas9-mediated knockout of clinically relevant  
735 alloantigenes in human primary T cells. *BMC Biotechnol* **21**, 9 (2021).
- 736 41. Brentjens, R. *et al.* CD19-targeted T cells rapidly induce molecular remissions in adults with  
737 chemotherapy-refractory acute lymphoblastic leukemia. *Sci Transl Med* **5**, 177ra38 (2013).
- 738 42. Tsai, S. Q. *et al.* CIRCLE-seq: a highly sensitive in vitro screen for genome-wide CRISPR–Cas9 nuclease off-  
739 targets. *Nature Methods* **14**, 607–614 (2017).
- 740 43. Magoč, T. & Salzberg, S. L. FLASH: fast length adjustment of short reads to improve genome assemblies.  
741 *Bioinformatics* **27**, 2957–2963 (2011).
- 742 44. Miller, N. A. *et al.* A 26-hour system of highly sensitive whole genome sequencing for emergency  
743 management of genetic diseases. *Genome Medicine* **7**, 1–16 (2015).
- 744 45. Chen, X. *et al.* Manta: Rapid detection of structural variants and indels for germline and cancer  
745 sequencing applications. *Bioinformatics* **32**, 1220–1222 (2016).
- 746 46. Genomics in the cloud : using Docker, GATK, and WDL in Terra - University of Wolverhampton.  
747 [https://librarysearch.wlv.ac.uk/discovery/fulldisplay/alma991002848267404901/44UOWO\\_INST:MAIN](https://librarysearch.wlv.ac.uk/discovery/fulldisplay/alma991002848267404901/44UOWO_INST:MAIN).
- 748 47. Ryan Poplin *et al.* Scaling accurate genetic variant discovery to tens of thousands of samples. *bioRxiv*  
749 201178 (2018) doi:10.1101/201178.

750 48. Love, M. I., Huber, W. & Anders, S. Moderated estimation of fold change and dispersion for RNA-seq  
751 data with DESeq2. *Genome Biology* **15**, 550 (2014).

752

753

754

755 **Figure 1 The Pin-point platform is a highly efficient technology for multiplex editing in T-cells.**

756 **A)** Schematic of the Pin-point base editing technology used in this manuscript. An SpCas9  
757 nickase (nCas9-UGI-UGI) binds to the gRNA, the recruiting RNA aptamer (MS2) fused to the  
758 gRNA recruits the effector module. The effector module is composed of a cytidine deaminase  
759 (rAPOBEC1) fused to the aptamer binding protein (MCP). The recruitment of the deaminase to  
760 the target site forms an active complex capable of editing target cytosine residues on the  
761 unpaired DNA strand within the CRISPR R-loop. **B)** Levels of C to T conversion of the target C at  
762 *B2M*, *CD52*, *TRAC* and *PDCD1* loci following co-delivery of Pin-point mRNAs and four target  
763 sgRNAs, as analysed by NGS seven days post electroporation. **C)** Levels of C to G or A conversion  
764 of the target C at *B2M*, *CD52*, *TRAC* and *PDCD1* loci following co-delivery of Pin-point mRNAs and  
765 four target sgRNAs, as analysed by NGS. **D)** Insertion (INS) and deletion (DEL) frequency at the  
766 target C at *B2M*, *CD52*, *TRAC* and *PDCD1* loci following co-delivery of Pin-point mRNAs and four  
767 target sgRNAs, as analysed by NGS. Data represented as mean  $\pm$  SD, n = 4 independent biological  
768 T-cell donors.

769 **Figure 2 Quantification of T cell target knockout in individual cells. A)** Frequency of CD52,  
770 TCRa/b, PD1, and B2M protein loss following co-delivery of Pin-point or SpCas9 mRNAs and their  
771 compatible four target sgRNAs, as analysed by flow cytometry seven days post electroporation.  
772 In this comparison, optimal gRNAs for SpCas9 have been used and these differ in their spacer  
773 sequence from the optimal Pin-point gRNAs (further details in the Method section). Protein loss  
774 is reported as normalised on pulse electroporated cells. **B)** Fractions of total live cells that were  
775 positive for 3 or less of three target proteins (B2M, CD52 and TCRa/b) following co-delivery of  
776 Pin-point or SpCas9 mRNAs and four target gRNAs, as analysed by flow cytometry seven days  
777 post electroporation. Control is mock electroporated T cells without RNA. **C)** Fold expansion of T

778 cells as measured by cell counts three days post co-delivery of Pin-point or SpCas9 mRNAs and 2,  
779 3 or 4 target gRNAs. Data represented as mean  $\pm$  SD, n = 2–4 independent biological T-cell  
780 donors. \*pvalue  $\leq$ 0.05, \*\*pvalue $\leq$ 0.01

781 **Figure 3 Assessment of DNA off-target editing and translocations. A-B)** On-/off-target activity  
782 of sgRNAs targeting *B2M*, *PDCD1*, *TRAC* or *CD52* genes, determined by rhAmpSeq NGS profiling  
783 of on-target and 100 off-target sites per gRNA identified by CHANGE-seq. The on-/off-target  
784 activity of each sgRNA was profiled with either the Pin-point base editor or SpCas9 and the  
785 percent editing (% base editing events (A) or % indels events (B)) determined in each case. Each  
786 dot depicts the maximal percentage editing at a given site in one human donor for control (mock  
787 electroporation, x axis) vs edit (edited sample, y axis) with an average coverage per panel of  
788 >35,000 reads. Blue dots highlight on-target editing, while red dots highlight validated off-target  
789 activity occurring in at least 0.5 % of reads (dotted lines) and in both human donors profiled. **C)**  
790 Percentage of Capture-seq sequencing reads marked as translocations by the DRAGEN Structural  
791 Variant (SV) Caller mapping to each sgRNA target site. Pin-point or SpCas9 mRNAs were  
792 delivered with four targeting sgRNAs. Control is mock electroporated T cells without RNA.  
793 Samples were analysed three days post electroporation. n=2 independent T cell donors.

794 **Figure 4 Effect of Pin-point base editing on RNA editing and transcription. A-B)** RNA C to U  
795 editing assessed by transcriptome sequencing in primary human T cells that were electroporated  
796 with Pin-point (nCAs9-UGI-UGI and rAPOBEC1-MCP) or nCAs9-UGI-UGI only mRNAs and the 4  
797 targeting sgRNAs against *B2M*, *CD52*, *TRAC* and *PDCD1* genes (A) or a scrambled non targeting  
798 sgRNA (B). Each dot represents one editing event. The total number of editing events is  
799 indicated above. **C)** Reads aligned to the Pin-point mRNA sequences (nCAs9-UGI-UGI and

800 rAPOBEC-MCP) in RNA samples from T cells electroporated with Pin-point mRNAs and the four  
801 targeting sgRNAs (*TRAC*, *B2M*, *CD52*, *PDCD1*) at different time points post electroporation.  
802 Individual samples were run through the GATK Best Practice for RNA-Seq Pipeline, where  
803 instead of aligning against the transcriptome, reads are aligned against the reference sequences  
804 (i.e. rAPOBEC1-MCP or nCas9-UGI-UGI) corresponding to that sample. As a result, a filtered  
805 alignment file (in BAM-format) and Variant Call Format (VCF) file was generated for each  
806 sample. Using the BAM files, read counts were determined for each component aligned against.

807 **D-I)** Scatter plots of gene expression levels ( $\log_2$  transformed TPM +1, TPM with a pseudocount  
808 of one added before log transformation) in primary human T cells electroporated with Pin-point  
809 mRNAs and either a scramble non-targeting (nt) sgRNA (D, E, F) or the four targeting sgRNAs  
810 (*TRAC*, *B2M*, *CD52*, *PDCD1*) (G, H,I) compared to control cells that received the pulse  
811 electroporation only (x-axis). DESeq2 analysis was performed on total mRNA collected at days 1  
812 (D, G), 3 (E, H) and 7 (F, I) post electroporation and was used to identify up- and down-regulated  
813 genes. Up- or down-regulated genes ( $p < 0.05$ ) with absolute  $\log_2$ -fold change  $\geq 1.5$  in gene  
814 expression (represented as  $\log_2$  transformed TPM +1) marked red and blue, respectively.  $r$   
815 indicates the Pearson correlation coefficient, calculated for log-transformed values on all genes.

816 **Figure 5 Generation of multiplex edited CAR-T cells by combining base editing by Pin-point**  
817 **system and lentiviral delivery of the CAR.** CAR-T cells were generated by lentivirus delivery of  
818 the CD19-CAR and subsequently edited by either the Pin-point base editor or SpCas9. **A)**  
819 Frequency of CD52, TCRa/b, PD1, and B2M protein loss following co-delivery of Pin-point or  
820 SpCas9 mRNAs and four target sgRNAs, as analysed by flow cytometry seven days post  
821 electroporation in CAR-T cells. In this comparison, optimal gRNAs for SpCas9 have been used  
822 and these differ in their spacer sequence from the optimal Pin-point gRNAs (further details in

823 the Method section). **B)** Frequency of CD19-CAR positive cells in the transduced T cell population  
824 after delivery of either Pin-point or SpCas9 reagents and in unedited cells. Control cells are T  
825 cells that have been mock transduced. **C)** Raji cells killing measured by flow cytometry after co-  
826 culture with CAR-T cells unedited or multi-edited with the Pin-point system or with SpCas9 at 1:1  
827 or 3:1 T cells: target cells ratios. Control cells are T cells that have been mock transduced. **D)**  
828 Levels of TNF $\alpha$  and INF $\gamma$  measured in the media of the co-culture at the 1:1 T cells: target cells  
829 ratio. Data represented as mean  $\pm$  SD, n = 2 independent biological T-cell donors.

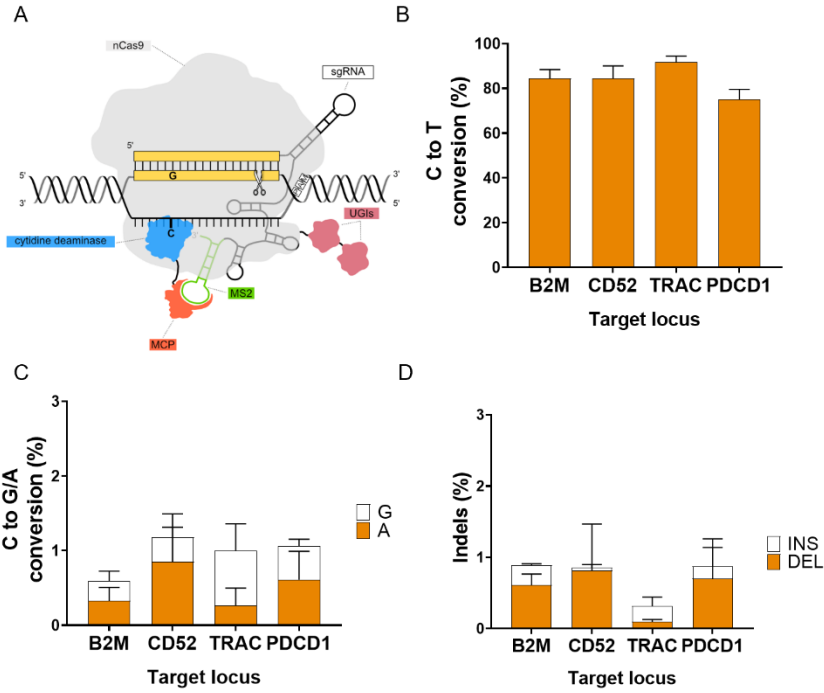
830 **Figure 6 Generation of multiplex edited CAR-T cells by simultaneous multiplex base editing**  
831 **knockout and locus specific knock-in with the Pin-point system. A)** Schematic showing the  
832 recruitment of the entire Pin-point system machinery by aptamer containing gRNAs on the site  
833 where the desired outcome is base editing (left) and of the nCas9 alone by aptamer-less gRNAs  
834 on the knock-in site (right). CAR-T cells were generated by knock-in of the CD19-CAR in the TRAC  
835 locus. Pin-point mRNAs have been co-delivered with aptamer containing sgRNAs directed to  
836 base edit *B2M*, *CD52* and *PDCD1* and 2 aptamer-less sgRNAs designed to target the exon1 of  
837 *TRAC* locus. Cells electroporated with SpCas9 mRNA received optimal gRNAs to knockout *B2M*,  
838 *CD52* and *PDCD1* by indels formation and one of the two gRNA designed to target the exon1 of  
839 *TRAC* locus. Shortly after electroporation, cells have been transduced with AAV6 carrying the  
840 CD19-CAR transgene flanked by the homology arms to the *TRAC* locus. **B)** Frequency of CD52,  
841 TCR $\alpha$ /b, PD1, and B2M protein loss following co-delivery of Pin-point or SpCas9 reagents and  
842 transduction with the AAV6-CAR as analysed by flow cytometry seven days post  
843 electroporation/transduction. **C)** Frequency of CD19-CAR positive cells in the T cell population  
844 after delivery of either Pin-point or SpCas9 reagents and transduction with the AAV6-CAR  
845 compared to non-transduced cells. **D)** Raji cells killing measured by calcein assay after co-culture



846 with T-cells unedited or multi-edited with the Pin-point system or with SpCas9 and transduced  
847 with AAV6-CAR compared to non-transduced cells at 1:1, 3:1 or 5:1 T cells: target cells ratios.  
848 Control cells are non-transduced cells. **E)** Levels of TNFa and INFg measured in the media of the  
849 co-culture at the 1:1 T cells: target cells ratio. Data represented as mean  $\pm$  SD, n = 2 independent  
850 biological T-cell donors.

851

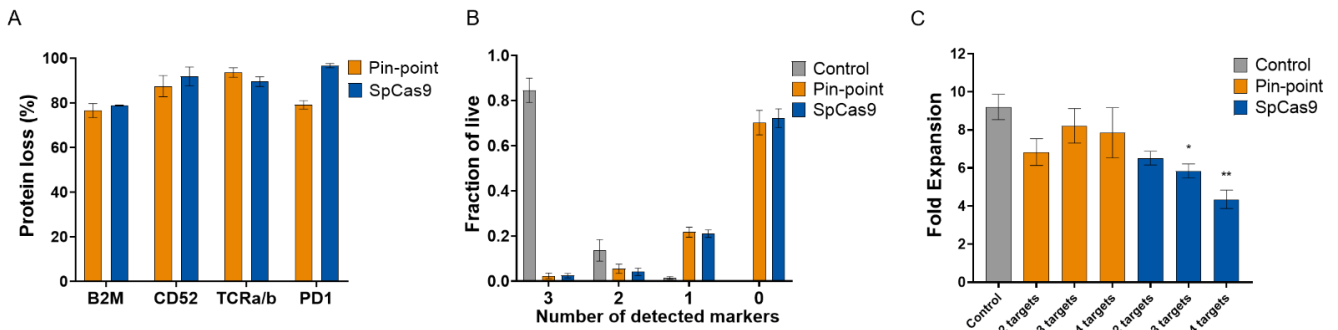
852 **Figures**



853

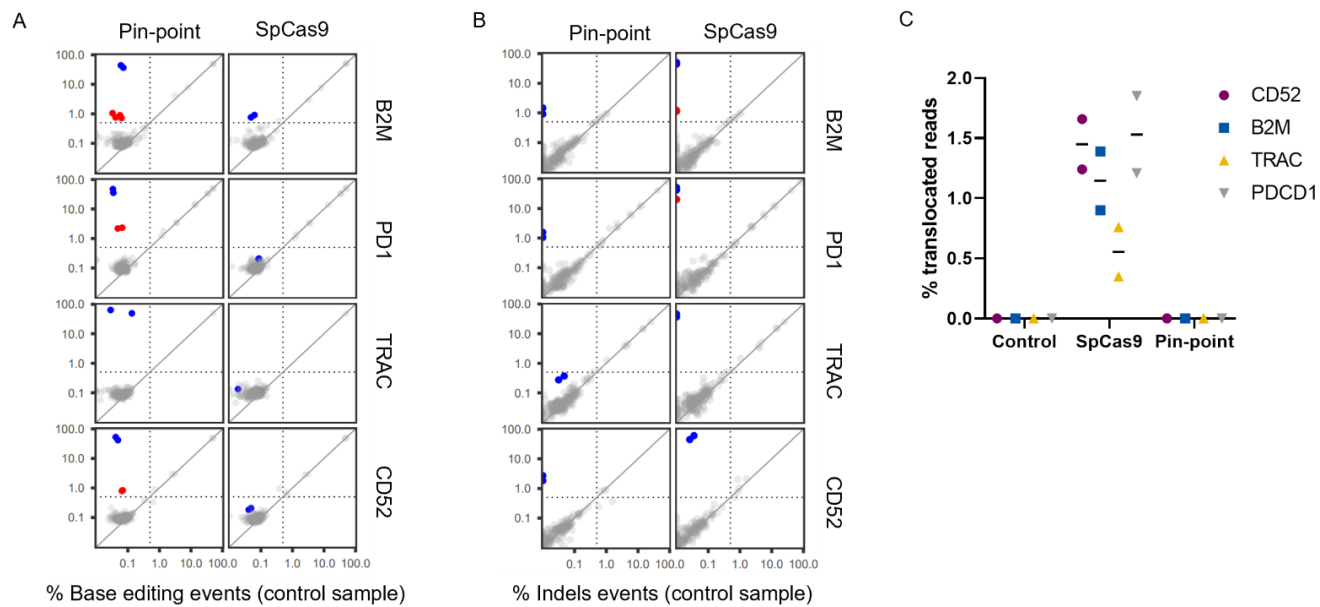
854 **Figure 1 The Pin-point platform is a highly efficient technology for multiplex editing in T-cells.**

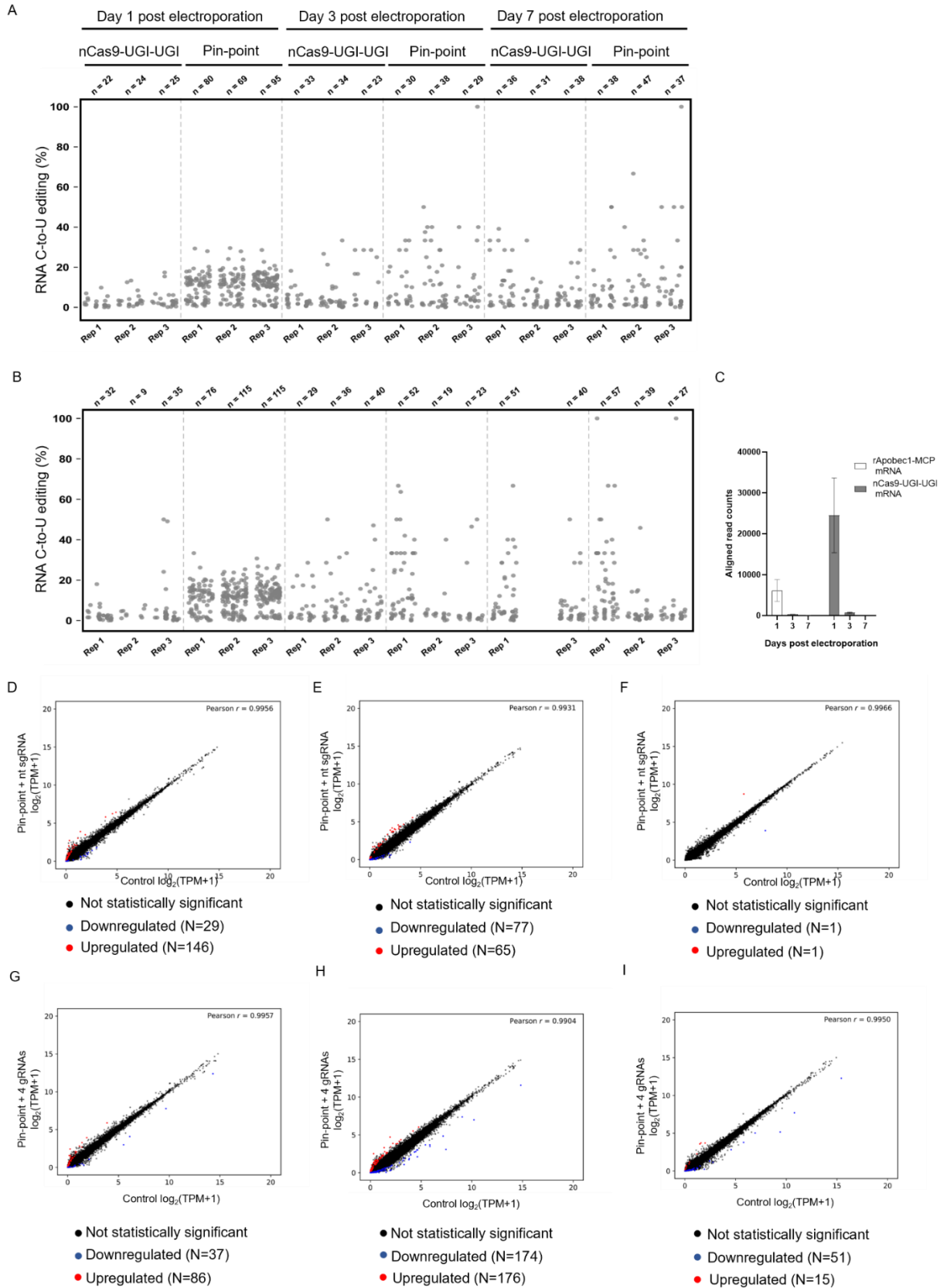
855



856

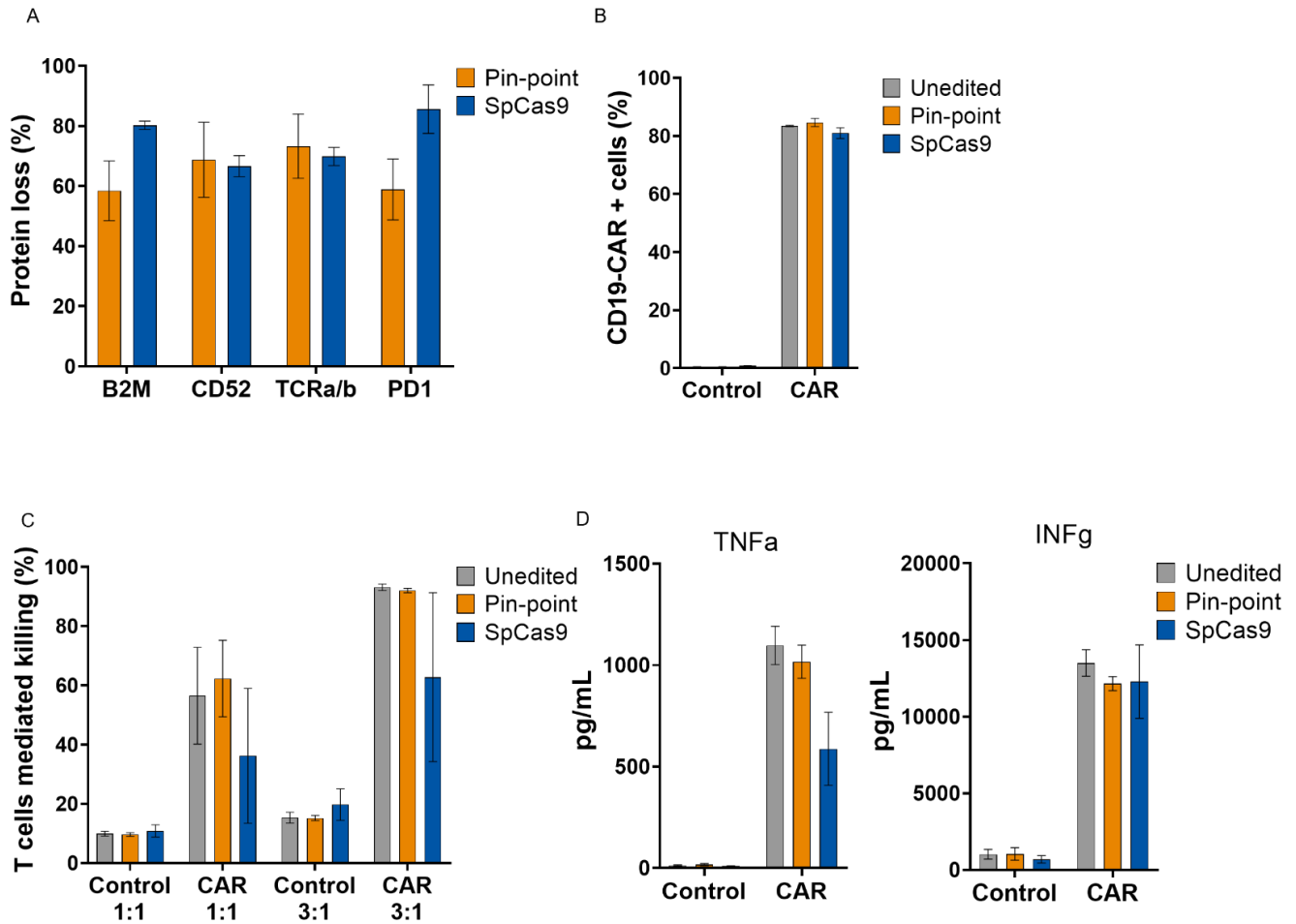
857 **Figure 2 Quantification of T cell target knockout in individual cells.**





860

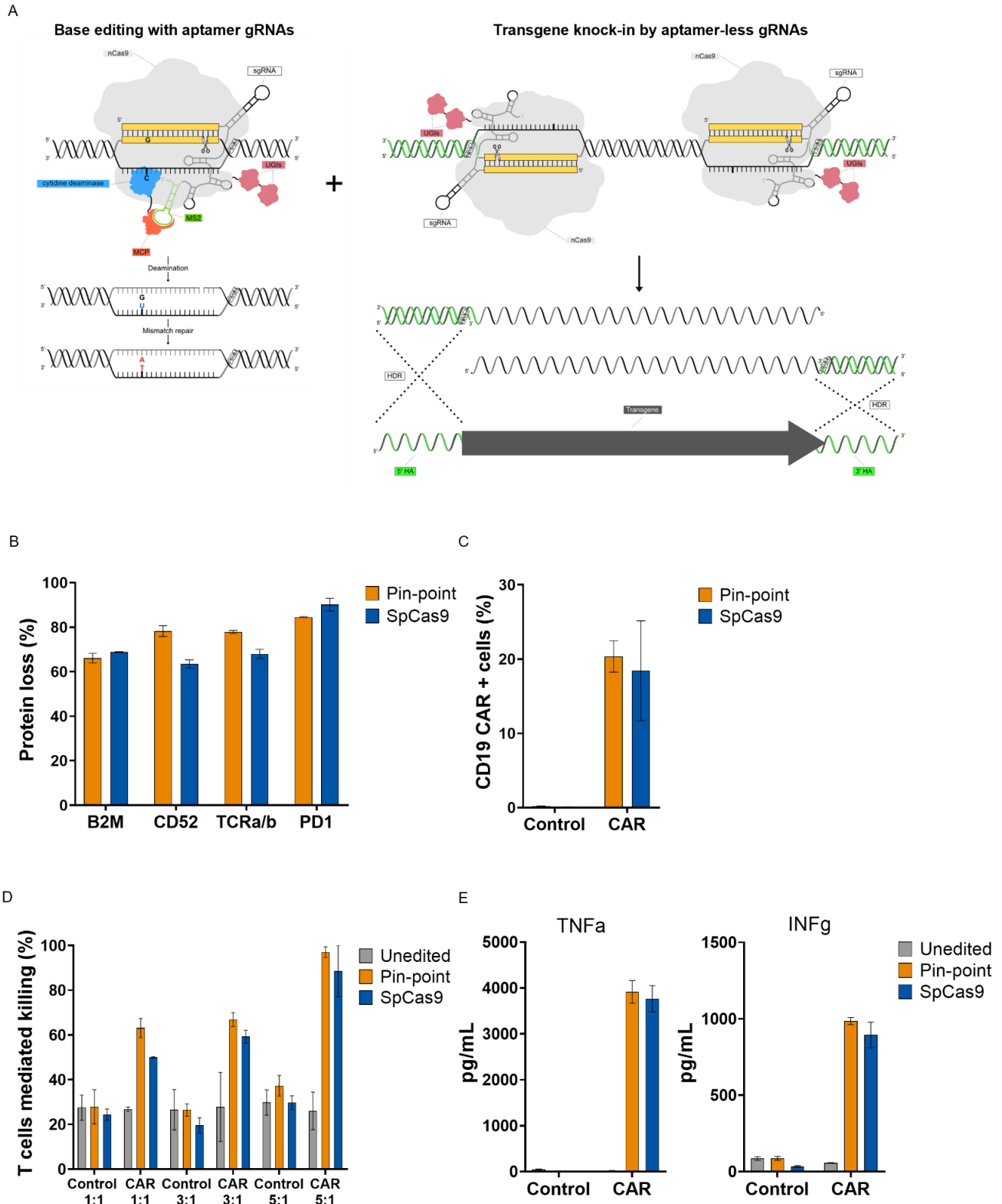
861 **Figure 4 Effect of Pin-point base editing on RNA editing and transcription.**



862

863 **Figure 5 Generation of multiplex edited CAR-T cells by combining base editing by Pin-point system**

864 **and lentiviral delivery of the CAR.**



865

866 **Figure 6 Generation of multiplex edited CAR-T cells by simultaneous multiplex base editing knockout**

867 **and locus specific knock-in with the Pin-point system**